Mersmann, F., Seynnes, O. R., Legerlotz, K., Arampatzis, A. (2018). Effects of tracking landmarks and tibial point of resistive force application on the assessment of patellar tendon mechanical properties in vivo. *Journal of Biomechanics, 71*, 176-182.

Effects of tracking landmarks and tibial point of resistive force application on the assessment of patellar tendon mechanical properties in vivo

Falk Mersmann[1,2], Olivier R. Seynnes[3], Kirsten Legerlotz[1,2], Adamantios Arampatzis[1,2]

[1]*Department of Training and Movement Sciences, Humboldt-Universität zu Berlin, Berlin, Germany,*

[2]*Berlin School of Movement Science, Berlin, Germany*

[3]*Department of Physical Performance, Norwegian School of Sports Sciences, Oslo, Norway*

Corresponding author:

Falk Mersmann

Humboldt-Universität zu Berlin

Department of Training and Movement Sciences

Philippstr. 13, Haus 11

10115 Berlin, Germany

Tel: +49 30 2093 46010

Fax: +49 30 2093 46046

E-Mail: falk.mersmann@hu-berlin.de

Article type: Original article

Key words: Tendon elongation; Ultrasound; Dynamometry; Pad position; Tracking features

Word count: 3986

Abstract

The different methods used to assess patellar tendon elongation *in vivo* may partly explain the large variation of mechanical properties reported in the literature. The present study investigated the effects of tracking landmark position and tibial point of resistive force application during leg extension in a dynamometer.

Nineteen adults performed isometric contractions using a proximal and distal shank pad position. Knee joint moments were calculated using an inverse dynamics approach. Tendon elongation was measured using the patellar apex and either the tibial tuberosity (T) or plateau (P) as tracking landmark.

Using P for tracking introduced a bias towards greater values of tendon elongation at all force levels from 100 N to maximum tendon force TFmax ($p<0.05$). The differences between landmarks considering maximum tendon strain were greater at the proximal shank pad position ($p<0.05$). Tendon stiffness was lower for P compared with T, but only in intervals up to 50% of TFmax ($p<0.05$). The agreement between T and P for stiffness calculated between 50% and TFmax was acceptable with the distal, but poor with the proximal pad position.

We demonstrated that using the tibia plateau and not the insertion as tracking landmark clearly affects the assessment of the force-elongation curve of the patellar tendon. However, using a distal point of resistive force application and calculating tendon stiffness between 50% and TFmax seems to yield an acceptable agreement between landmarks. These findings have important implications for the assessment of tendon properties in vivo and cross-study comparisons.

Introduction

It is well established that the mechanical properties of tendons play a crucial role for movement performance of musculoskeletal systems, since they determine the transmission of muscle force to the skeleton and allow for the storage and release of mechanical strain energy (Biewener et al., 1998; Roberts, 1997). In view of the epidemiology of tendon injuries (Järvinen, 1992), the association of tendon mechanical properties and pathophysiological mechanisms is also of interest for the scientific community and precisely estimating maximal tendon strain and stiffness could be of clinical relevance (LaCroix et al., 2013; Wren et al., 2003). The mechanical properties of tendons are determined based on their force-elongation behaviour (Butler et al., 1978), which has traditionally been studied using *in vitro* tensile testing (Benedict et al., 1968; Johnson et al., 1994; Woo et al., 1980). The introduction of an ultrasound-based approach to determine the elongation of tendon-aponeurosis complexes (Fukashiro et al., 1995; Maganaris and Paul, 1999) lay the ground for an increasing scientific interest in human *in vivo* tendon adaptation (Arampatzis et al., 2007; Kongsgaard et al., 2007; Reeves et al., 2003; Seynnes et al., 2009), muscle-tendon interaction (Fukunaga et al., 2002; Lichtwark et al., 2007; Nikolaidou et al., 2017), influence of tendon mechanical properties on human movement performance (Arampatzis et al., 2006; Bojsen-Møller et al., 2005; Karamanidis and Arampatzis, 2005; Stafilidis and Arampatzis, 2007) and their relation to injury (Arya and Kulig, 2010; Child et al., 2010; Helland et al., 2013).

Soon attempts were made to determine the mechanical properties of the patellar tendon *per se* as well (Hansen et al., 2006; Reeves et al., 2003), which involves the measurement of joint moments around the knee or a resultant exerted force and tendon elongation during muscle contractions. The latter is achieved by tracking the displacement of the tendon origin and insertion at the patellar apex and tibial tuberosity in the ultrasound images (O'Brien et al., 2010; Schulze et al., 2012). This, however, is only possible with ultrasound transducers visualizing both landmarks in a single field of view during the contraction (i.e. linear arrays with an approximate minimum length of 8 cm). When only short transducers are available, it is common that a prominent bony landmark close to the tibia plateau is used for tracking (Carroll et al., 2008; Kongsgaard et al., 2007; Kösters et al., 2014; Seynnes et al., 2011), based on the assumption that its displacement in the longitudinal axis of the tendon is representative of tendon elongation. Yet during knee extension contractions in the open kinetic chain, a tilt of the tibia is commonly observed in the ultrasound recordings (Seynnes et al., 2015). This means that the displacement of the insertion site is influenced by both a translational and rotational component and, therefore, the displacement of any other point distant to the insertion site that is caused by the tibia sagittal plane rotation and measured along the longitudinal axis of the tendon is different compared to the insertion site itself (see also figure 1, panel B). Therefore, the assessment of patellar tendon elongation based on the displacement of a landmark at the tibia plateau is likely to be associated with a measurement bias depending on the magnitude of tibia tilt during the isometric contractions. The movement of the tibia relative to the femur can be influenced by the point of resistive force application at the shank. Moving the point of resistive force application proximally increases the load on the posterior cruciate ligament due to a progressing posterior shift of the tibia plateau (Zavatsky et al., 1994). However, it is to date unknown how this affects the measurement of patellar tendon elongation based on ultrasound recordings. Therefore, the objective of the present study was to investigate how the choice of the tracking landmark and point of resistive force application influences the assessment of patellar tendon mechanical properties *in vivo*. We hypothesised that tracking the displacement of a landmark at the tibia plateau would lead to an overestimation of tendon elongation and, thus, underestimation of tendon stiffness, due to the additional displacement of the landmark induced by the tilt of the tibia during isometric contractions. We further expect both the tibia tilt and the associated bias on the elongation measurement be more pronounced with a proximal compared to a distal point of resistive force application.

Methods

Participants

Twenty-five healthy adults from the university population volunteered to participate in the present study, which was conducted in accordance with the recommendations of the local university ethics committee and with written informed consent from all subjects. Six subjects needed to be excluded due to ultrasound artefacts during image acquisition (n = 3), inability to follow through the whole experimental protocol (n = 1) or ultrasound probe movement artefacts that were detected in post-processing (n = 2). Average age, body height and body mass of the remaining 19 participants were 25 ± 4 years, 176 ± 10 cm and 69 ± 12 kg, respectively.

Experimental protocol and data acquisition

Following a standardised warm-up of five minutes of ergometer cycling, the participants were seated and fixated on a dynamometer (Biodex Medical System 3, Shirley, NY, USA) with the knee joint angle at 90° and the trunk angle at 85° (0° = full knee or hip extension; values refer to the angle determined by the dynamometer). The dynamometer shank pad was positioned in random order at 60% or 80% tibia length (from proximal to distal; measured between the medial tibia plateau and malleolus). For the use of inverse dynamics in the calculation of knee joint moments (see Arampatzis et al., 2004 for details), six reflective markers were fixed to the following anatomical landmarks: greater trochanter, lateral and medial femoral epicondyles and malleoli, and second metatarsal head. For estimating the contribution of antagonist activity to the resultant joint moments, two bipolar surface electrodes (Blue Sensor N, Ambu GmbH, Bad Nauheim, Germany) were fixed over the mid-portion of the muscle belly of the lateral head of the biceps femoris with an inter-electrode distance of 2 cm after shaving and cleaning the skin. The kinematic data were recorded using a Vicon motion capture system (version 1.7.1; Vicon Motion Systems, Oxford, UK) integrating eight cameras operating at 250 Hz. The electromyographic (EMG) data were captured at 1,000 Hz (Myon m320RX; Myon, Baar, Switzerland) and transmitted to the Vicon system via a 16-channel A-D converter. A 10-cm linear ultrasound probe (7.5 MHz; My Lab60; Esaote, Genova, Italy; probe: linear array (LA923), depth: 7.4 cm, focal point: 0.9 and 1.9) was fixed in a modified knee brace overlying the patellar tendon in the sagittal plane, capturing the elongation of the tendon during contractions at 25 Hz. A schematic of the experimental setup, including a representative ultrasound image of the patellar tendon and an illustration of both the elongation analysis as well as a model of how tibia tilt could affect the elongation measurement is shown in figure 1.

After ten submaximal isometric knee extension contractions as additional warm-up and familiarisation, the subjects performed one maximum voluntary contraction (MVC) and two blocks of five isometric ramp contractions, where the participants gradually increased contraction intensity up to 90% of their MVC in about five seconds. A screen set-up in front of the dynamometer provided online feedback about the moment measured at the dynamometer. Every ramp contraction in each block was preceded by five preconditioning contractions at 40% MVC (Maganaris, 2003). An additional passive trial (i.e. passive knee extension driven by the dynamometer at 5°/s with the shank of the participants fixed to the dynamometer lever pad) was recorded to account for moments due to gravity (Arampatzis et al., 2004) in the inverse dynamics approach. Further, two trials of knee flexions were captured to establish an EMG-activity knee flexion moment relationship for estimating the contribution of antagonistic muscles to the resultant joint moments (see Mademli et al., 2004 for details). Subsequently, the dynamometer shank pad position was changed to the other target position (i.e. 60% or 80% of tibia length) for the second block of five ramp contractions as well as the respective passive trial and the two knee flexion contractions.

Knee joint moments and tendon mechanical properties

The stiffness of the patellar tendon was derived from the force-elongation relationship during the isometric ramp contractions. Tendon force was calculated by dividing the knee extension moments – determined with the inverse dynamics approach suggested by Arampatzis and colleagues (2004) and considering antagonistic activity (Kellis and Baltzopoulos, 1997; Mademli et al., 2004) – by the tendon lever arm, which in turn was predicted using anthropometric data (Mersmann et al., 2016) and adjusted to the respective knee joint angle position based on the data by Herzog and Read (1993).

Tendon elongation during the ramp contraction was assessed by measuring the displacement of the deep origin at the patellar apex and both the deep insertion at the tibial tuberosity and a prominent landmark close to the edge of the tibia plateau using a semi-automatic tracking software (Tracker Video Analysis and Modeling Tool V. 4.92, Open Source Physics, Aptos, California, USA). When using the tibial tuberosity, elongation was measured as vector between the two landmarks, which also was defined as the longitudinal axis of the tendon. When tracking the tibia plateau, the displacement along this longitudinal axis was considered for the elongation measurement (figure 1, panel A) to account for the misalignment between the vector connecting the landmarks (plateau and the patella apex) and the patellar tendon. To account for tracking errors, for example due to relative probe movement with respect to the bony structures, the digitalisations were considered valid if the R^2 of a second order polynomial fit of the resultant force-elongation curve was at least 0.9 (Seynnes et al., 2015). If less than three trials fulfilled the criteria, the participant was excluded (n = 2). For all participants included in the final analysis, all 5 trials per condition were available for further analysis, which ensures an excellent reliability of the patellar tendon elongation measurement (Schulze et al., 2012). The force-elongation curves of each pad-position condition (i.e. 5 trials) were averaged up to a common maximum tendon force of the ramp contractions in both conditions (TF_{max}). Tendon stiffness was calculated in 10%-intervals of relative tendon force (relative to the individual maximum tendon force exerted during the MVC assessment: TF_{MVC}) as well as between 50% TF_{MVC} and TF_{max} as slope of a linear regression. TF_{MVC} was used to determine relative tendon force thresholds due to the marked differences in the capability of the individual participants to exert force during the ramp contractions (TF_{max} ranged between 73% and 95% TF_{MVC}). As an indication for tibia tilt, we calculated the angle between the lower border of the patellar tendon and the anterior intercondylar area (see figure 1). All outcome parameters related to the ramp contractions with the two pad position conditions (e.g. maximum elongation and strain, knee angular change, antagonistic moment, tibia tilt) were evaluated at TF_{max} and the average of the five trials was considered for analysis.

Statistics

All statistical procedures were carried out in SPSS (version 20.0; IBM, Armonk, NY, USA). We performed an analysis of variances for repeated measures (RM ANOVA) with the within-subject factors *pad position* (i.e. proximal, distal) *tracking landmark* (i.e. tuberosity, plateau) and *force level* (i.e. from 100 N to 1800 N every 100 N and TF_{max}) on the tendon force-elongation data. Normality of the data was tested using the Shapiro-Wilk test and Mauchly's test was applied to test sphericity. Due to a violation of both assumptions at some of the force levels, we applied the Huynh-Feldt correction, as it has demonstrated robust error I control upon violation of normality and sphericity at similar sample sizes and factor levels (Oberfeld and Franke, 2012). In case of significant landmark- or pad position-by-force level interactions, we used the Wilcoxon signed-rank test and Bonferroni adjustment to test differences between landmarks or pad positions at each force level, respectively. A similar approach was taken to analyse tendon stiffness calculated in 10%-intervals of TF_{MVC}. With regard to maximum strain and stiffness calculated between 50% TF_{MVC} and TF_{max}, no force level factor was applied in the RM ANOVA. Considering all other parameters (resting knee joint angle and angular rotation, antagonistic moment, tibia tilt), the two pad position conditions were compared with students t-tests after testing for normality. The alpha level for all tests was 0.05 and effect sizes *f* were calculated for significant effects, interactions and differences using G*Power (Version 3.1.6; HHU, Düsseldorf, Germany; (Faul et al., 2007)). Effect sizes of $0.1 \leq f < 0.25$ can be considered as small, $0.25 \leq f < 0.5$ as medium and $f \geq 0.5$ as large (Cohen, 2013). To examine the agreement between the results obtained from using either the tibia plateau or tuberosity as tracking landmark we used Bland-Altman plots (Bland and Altman, 1986). The agreements were considered *good*, if their limits (mean ±1.96 standard deviation of the differences between methods) were smaller than the differences that can be expected following interventions or between cohorts, *acceptable* in case of similar limits and *poor* in case of greater limits.

Results

There was no difference in the resting knee joint angle ($p = 0.86$) or in the moment due to the activation of the antagonistic knee flexors during the maximum ramp contractions ($p = 0.86$), yet a significantly greater angular change from rest to maximum in the proximal compared to the distal pad position condition ($p < 0.001, f = 1.43$; table 1). Similarly, the tibia tilt (i.e., angular change between the tendon and anterior intercondylar area; see figure 1) was significantly greater during contractions with the proximal pad position ($p < 0.001, f = 0.84$; table 1). Figure 2 illustrates the tibia tilt as a function of relative tendon force for both pad positions, respectively.

TF_{MVC} and TF_{max} were on average 4119 ± 1114 N and 3401 ± 842 N (i.e. ~83% TF_{MVC}), respectively. Figure 3 illustrates the force-elongation behaviour yielded by the analysis using the two landmarks and pad position conditions for every 100 N of tendon force and TF_{max}. There was a main effect of landmark ($p < 0.001, f = 1.51$), force level ($p < 0.001, f = 2.92$) and a significant landmark-by-force level interaction ($p < 0.001, f = 0.99$), yet no significant main effect of pad position ($p = 0.468$) or interaction with force level ($p = 0.798$). *Post hoc* testing revealed significant differences between landmarks for all force levels ($p < 0.001$, $0.48 \leq f \leq 0.67$), indicating an overestimation of elongation when using the plateau as tracking landmark with increasing effect sizes up to 1200 N. Similarly, there was a significant main effect of tracking landmark ($p < 0.001, f = 1.16$), force level ($p < 0.001, f = 1.19$), and landmark-by-force level interaction ($p < 0.001, f = 1.03$), on stiffness calculated in 10%-intervals of TF_{MVC}, while no significant main effect of pad position ($p = 0.901$) or interaction with force level (p = 0.054) was present (figure 4). *Post hoc* comparisons showed significant differences between landmarks in the intervals up to 50% TF_{MVC} ($p \leq 0.002$, $0.35 \leq f \leq 0.62$), while the differences in the intervals 50-60% and 60-70% TF_{MVC} were not statistically significant ($p \geq 0.06$).

Maximum strain demonstrated a significant effect of landmark ($p < 0.001$, $f = 1.40$) with greater maximum strain values when using the plateau as tracking landmark, while no significant main effect of the pad position was present (p = 0.41; figure 5A). A significant landmark-by-pad position interaction (p = 0.003, $f = 0.81$) and *post hoc* analysis indicated greater differences between landmarks at the proximal pad position (p = 0.013) as well as greater differences between pad positions for the analysis using the plateau as landmark (p = 0.013). The Bland-Altman plots in figure 6 illustrate the poor agreement between maximum strain obtained from the analysis using the landmark at the tibia plateau and tuberosity at the distal (limits of agreement of 2.02 to -4.12%; A) and proximal pad position (limits of agreement of 0.54 to -5.24%; B), respectively. Though there was neither a significant main effect of landmark or pad position nor a landmark-by-pad position interaction on stiffness calculated between 50% TF_{MVC} and TF_{max} (figure 5B), the agreement between methods was only acceptable at the distal pad position (limits of agreement of 249 N/mm to -308 N/mm; figure 5C) and poor at the proximal pad position (limits of agreement of 704 to -558 N/mm; figure 6D).

Discussion

The present study investigated the effect of the choice of tracking landmark and point of resistive force application at the shank on the assessment of patellar tendon elongation during isometric contractions *in vivo*. In line with our hypotheses, we found that tracking a bony landmark close to the tibia plateau overestimates the elongation of the tendon throughout the whole force-elongation curve and results in lower values of the first derivative of the force elongation curve up to 50% of maximum tendon force. A proximal position of the point of resistive force application appears to amplify this bias and compromises the agreement between tracking landmarks.

Our hypothesis that using a landmark at the tibia plateau instead of the tendon insertion at the tibial tuberosity would overestimate tendon elongation was based on the common observation of a tibia tilt during isometric contractions in the open kinetic chain (Seynnes et al., 2015). In the present study, the tilt of the tibia was determined as change in the angle between the tendon and the anterior intercondylar area (α), as a change in this angle leads to a displacement of the tibia plateau along the longitudinal axis of the tendon that is not representative of the actual tendon elongation (see figure, panel B). The bias associated with this angular rotation (ΔL) can be calculated as $\Delta L = r \cdot cos(\alpha) - r \cdot cos(\alpha + \Delta\alpha)$, under the simplified assumption that the vector r from the landmark at the tuberosity to the one at the plateau is constant, and it explained 44% of the variance of the between-method differences in maximum elongation ($r = 0.66$; $p < 0.001$).

The major contraction-induced tilt of the tibia can be observed up to about 50% TF_{MVC}, which explains both that a) the elongation measured at a given force differs substantially between the two landmarks already at low force levels and b) that stiffness calculated at force levels below 50% TF_{MVC} is significantly lower when the plateau was used for tracking instead of the tuberosity. This is an important finding with respect to the interpretation of experimental results as well as for the conduction of future *in vivo* studies investigating the mechanical properties of the patellar tendon. For example, tendon strain during maximum isometric contractions can be used as a marker for the mechanical demand placed upon the tendon by the working muscle, as there is convincing evidence that ultimate strain can be assumed to be more or less constant (Abrahams, 1967; LaCroix et al., 2013; Loitz et al., 1989; Shepherd and Screen, 2013). Recent *in vivo* studies on humans support the notion that tendon overuse injury might be related to increased tendon strain during high-effort muscle contractions (Arya and Kulig, 2010; Child et al., 2010; Mersmann et al., 2016; 2017). Though the outcomes of tracking of the patellar plateau have shown to be reproducible (Hansen et al., 2006; Kösters et al., 2014), maximum tendon strain values were significantly greater compared to those measured using the actual insertion at the tuberosity. When the precision of measuring maximum tendon strain *in vivo* is compromised due to tibia sagittal plane rotation, it might not be possible to identify associations between maximum *in vivo* tendon strain other outcome parameters. This limitation also needs to be considered when investigating tendon stiffness at lower levels or tendon force, which might be of scientific interest considering the different micromechanical mechanisms underlying the force-elongation behaviour of tendons at different force levels (Screen et al., 2004). Surprisingly, maximum strain values (of young recreationally active adults) reported by authors that used the displacement of the plateau in the assessment of patellar tendon elongation (Carroll et al., 2008; e.g. 5.8-6.9%; Hansen et al., 2006; Kongsgaard et al., 2007; Seynnes et al., 2013) are actually lower compared to those obtained in the present study when tracking the tuberosity (i.e. 7.3% at the distal pad position). However, this might be related to the respective tracking procedures, since studies that used the same automatic tracking algorithms as applied in the present study reported similar strain values as we found as a result of plateau-tracking (8.3% vs. 8.2-8.9%; Kösters et al., 2014; Wiesinger et al., 2016).

In accordance with models for cruciate ligament loading (Zavatsky et al., 1994), shifting the point of resistive force application proximally led to significantly greater angular rotation of the knee joint and tibia tilt at a similar knee extension moment. The magnitude of the reactive force at the shank pad increases at a given resultant knee joint moment when the pad is located more proximally, as the product of the reactive force and its lever arm (with respect to the knee joint) needs to be in equilibrium with the moment exerted at the knee during isometric muscle contractions. This increase of reactive force is likely to contribute to the posterior shift of the plateau and increasing sagittal plane rotation as well. In consequence of the increase of tibia tilt, the overestimation of maximum tendon strain upon the use of the plateau for tracking was significantly greater (indicated by the tracking landmark-by-pad position interaction) and we found a marked impairment of the agreement with tracking the tuberosity in the measurement of tendon stiffness at the proximal shank pad position. It is interesting to note that shifting the point of resistive force application proximally did not introduce a systematic bias but increased the spread of the differences in stiffness between the two tracking landmarks. It could well be that an increase in angular rotation and tibia tilt during isometric contractions (even above 50% of TF_{MVC}) is associated with out-of-plane movements of the ultrasound probe, which introduces different tracking errors at the two sites (Seynnes et al., 2015). However, even at the more favourable pad position condition, the limits of agreement of 22% and -27% indicate considerable differences in stiffness calculated from the elongation measured using the two tracking methods. Assuming that random tracking errors occur using both landmarks, the tibia tilt generates an additional uncertainty affecting only the elongation measurement at the plateau. It is thus likely that a given effect that is present during an *in vivo* investigation remains concealed or can only be detected at greater sample sizes due to a reduced precision of that approach compared to tuberosity-tracking. Nevertheless, group mean values of stiffness at high force levels seem to be similar and allow comparison of values obtained using both tracking-approaches, as the major contraction-induced tibia tilt occurs up to 50% TF_{MVC} and reaches a plateau afterwards.

In conclusion, the choice of tracking landmark affects the measurement of patellar tendon elongation during isometric contractions *in vivo*. Tracking a bony landmark close to the tibia plateau introduces a measurement bias towards greater elongation of the tendon throughout the whole force-elongation curve due to its sensitivity to the tibia tilt that occurs during isometric knee extension contractions. Consequently, the approach yields lower values of the first derivative of the force elongation curve up to 50% of maximum tendon force, which corresponds well with the tibia tilt as a function of exerted force. A proximal position of the point of resistive force application appears to amplify the measurement-bias of the plateau-tracking and compromises the agreement to the results from tracking the tuberosity. However, the use of a distal point of resistive force application together with a calculation of tendon stiffness at higher tendon force levels yields results that allow for cross-study comparisons. These results have important implications for the design of future *in vivo* studies on the mechanical properties of the patellar tendon as well as the interpretation of the results published in the literature.

Conflict of interest statement

All authors disclose any financial and personal relationships with other people or organisations that could inappropriately influence (bias) the study.

Acknowledgements

The authors thank Arne Schlausch for supporting the data analysis and Arno Schroll for sharing his expertise on the statistical analysis.

References

Abrahams, M., 1967. Mechanical behaviour of tendon in vitro. A preliminary report. Med. Biol. Eng. 5, 433–443.

Arampatzis, A., De Monte, G., Karamanidis, K., Morey-Klapsing, G., Stafilidis, S., Brüggemann, G.-P., 2006. Influence of the muscle-tendon unit's mechanical and morphological properties on running economy. J. Exp. Biol. 209, 3345–3357.

Arampatzis, A., Karamanidis, K., Albracht, K., 2007. Adaptational responses of the human Achilles tendon by modulation of the applied cyclic strain magnitude. J. Exp. Biol. 210, 2743–2753.

Arampatzis, A., Karamanidis, K., De Monte, G., Stafilidis, S., Morey-Klapsing, G., Bruggemann, G., 2004. Differences between measured and resultant joint moments during voluntary and artificially elicited isometric knee extension contractions. Clin. Biomech. 19, 277–283.

Arya, S., Kulig, K., 2010. Tendinopathy alters mechanical and material properties of the Achilles tendon. J. Appl. Physiol. 108, 670–675.

Benedict, J.V., Walker, L.B., Harris, E.H., 1968. Stress-strain characteristics and tensile strength of unembalmed human tendon. J. Biomech. 1, 53–63.

Biewener, A.A., Konieczynski, D.D., Baudinette, R.V., 1998. In vivo muscle force-length behavior during steady-speed hopping in tammar wallabies. J. Exp. Biol. 201, 1681–1694.

Bland, J.M., Altman, D.G., 1986. Statistical methods for assessing agreement between two methods of clinical measurement. Lancet 1, 307–310.

Bojsen-Møller, J., Magnusson, S.P., Rasmussen, L.R., Kjaer, M., Aagaard, P., 2005. Muscle performance during maximal isometric and dynamic contractions is influenced by the stiffness of the tendinous structures. J. Appl. Physiol. 99, 986–994.

Butler, D.L., Grood, E.S., Noyes, F.R., Zernicke, R.F., 1978. Biomechanics of ligaments and tendons. Exerc. Sport Sci. Rev. 6, 125–181.

Carroll, C.C., Dickinson, J.M., Haus, J.M., Lee, G.A., Hollon, C.J., Aagaard, P., Magnusson, S.P., Trappe, T.A., 2008. Influence of aging on the in vivo properties of human patellar tendon. J. Appl. Physiol. 105, 1907–

1915.

Child, S., Bryant, A.L., Clark, R.A., Crossley, K.M., 2010. Mechanical properties of the achilles tendon aponeurosis are altered in athletes with achilles tendinopathy. Am. J. Sports Med. 38, 1885–1893.

Cohen, J., 2013. Statistical Power Analysis for the Behavioral Sciences. Routledge.

Faul, F., Erdfelder, E., Lang, A.-G., Buchner, A., 2007. G*Power 3: a flexible statistical power analysis program for the social, behavioral, and biomedical sciences. Behav. Res. Methods 39, 175–191.

Fukashiro, S., Itoh, M., Ichinose, Y., Kawakami, Y., Fukunaga, T., 1995. Ultrasonography gives directly but noninvasively elastic characteristic of human tendon in vivo. Eur J. Appl. Physiol. O 71, 555–557.

Fukunaga, T., Kawakami, Y., Kubo, K., Kanehisa, H., 2002. Muscle and tendon interaction during human movements. Exerc. Sport Sci. Rev. 30, 106–110.

Hansen, P., Bojsen-Moller, J., Aagaard, P., Kjaer, M., Magnusson, S., 2006. Mechanical properties of the human patellar tendon, in vivo. Clin. Biomech. 21, 54–58.

Helland, C., Bojsen-Moller, J., Raastad, T., Seynnes, O.R., Moltubakk, M.M., Jakobsen, V., Visnes, H., Bahr, R., 2013. Mechanical properties of the patellar tendon in elite volleyball players with and without patellar tendinopathy. Br. J. Sports Med. 47, 862–868.

Herzog, W., Read, L.J., 1993. Lines of action and moment arms of the major force-carrying structures crossing the human knee joint. J. Anat. 182 (Pt 2), 213–230.

Järvinen, M., 1992. Epidemiology of tendon injuries in sports. Clin. Sports Med. 11, 493–504.

Johnson, G.A., Tramaglini, D.M., Levine, R.E., Ohno, K., Choi, N.Y., Woo, S.L., 1994. Tensile and viscoelastic properties of human patellar tendon. J. Orthop. Res. 12, 796–803.

Karamanidis, K., Arampatzis, A., 2005. Mechanical and morphological properties of different muscle-tendon units in the lower extremity and running mechanics: effect of aging and physical activity. J. Exp. Biol. 208, 3907–3923.

Kellis, E., Baltzopoulos, V., 1997. The effects of antagonist moment on the resultant knee joint moment during isokinetic testing of the knee extensors. Eur. J. Appl. Physiol. O 76, 253–259.

Kongsgaard, M., Reitelseder, S., Pedersen, T.G., Holm, L., Aagaard, P., Kjaer, M., Magnusson, S.P., 2007. Region specific patellar tendon hypertrophy in humans following resistance training. Acta Physiol. (Oxf.) 191, 111–121.

Kösters, A., Wiesinger, H.P., Bojsen-Moller, J., Muller, E., Seynnes, O.R., 2014. Influence of loading rate on patellar tendon mechanical properties in vivo. Clin. Biomech. (Bristol, Avon) 29, 323–329.

LaCroix, A.S., Duenwald-Kuehl, S.E., Lakes, R.S., Vanderby, R., 2013. Relationship between tendon stiffness and failure: a metaanalysis. J. Appl. Physiol. 115, 43–51.

Lichtwark, G.A., Bougoulias, K., Wilson, A.M., 2007. Muscle fascicle and series elastic element length changes along the length of the human gastrocnemius during walking and running. J. Biomech. 40, 157–164.

Loitz, B.J., Zernicke, R.F., Vailas, A.C., Kody, M.H., Meals, R.A., 1989. Effects of short-term immobilization versus continuous passive motion on the biomechanical and biochemical properties of the rabbit tendon. Clin. Orthop. Relat. Res. 265–271.

Mademli, L., Arampatzis, A., Morey-Klapsing, G., Bruggemann, G., 2004. Effect of ankle joint position and electrode placement on the estimation of the antagonistic moment during maximal plantarflexion. J. Electromyogr. Kines. 14, 591–597.

Maganaris, C.N., 2003. Tendon conditioning: artefact or property? Proc. R. Soc. Lond. B.: Biol. Sci. 270, S39–S42.

Maganaris, C.N., Paul, J.P., 1999. In vivo human tendon mechanical properties. J. Physiol. (Lond.) 521 Pt 1, 307–313.

Mersmann, F., Bohm, S., Schroll, A., Marzilger, R., Arampatzis, A., 2016. Athletic Training Affects the Uniformity of Muscle and Tendon Adaptation during Adolescence. J. Appl. Physiol. 121, 893–899.

Mersmann, F., Charcharis, G., Bohm, S., Arampatzis, A., 2017. Muscle and Tendon Adaptation in Adolescence: Elite Volleyball Athletes Compared to Untrained Boys and Girls. Front. Physiol. 8, 417.

Nikolaidou, M.E., Marzilger, R., Bohm, S., Mersmann, F., Arampatzis, A., 2017. Operating length and velocity of human M. vastus lateralis fascicles during vertical jumping. R. Soc. Open Sci. 4, 170185.

O'Brien, T.D., Reeves, N.D., Baltzopoulos, V., Jones, D.A., Maganaris, C.N., 2010. Mechanical properties of the patellar tendon in adults and children. J. Biomech. 43, 1190–1195.

Oberfeld, D., Franke, T., 2012. Evaluating the robustness of repeated measures analyses: The case of small sample sizes and nonnormal data. Behav. Res. Methods 45, 792–812.

Reeves, N.D., Maganaris, C.N., Narici, M.V., 2003. Effect of strength training on human patella tendon mechanical properties of older individuals. J. Physiol. (Lond.) 548, 971–981.

Roberts, T.J., 1997. Muscular Force in Running Turkeys: The Economy of Minimizing Work. Science 275, 1113–1115.

Schulze, F., Mersmann, F., Bohm, S., Arampatzis, A., 2012. A wide number of trials is required to achieve acceptable reliability for measurement patellar tendon elongation in vivo. Gait & Posture 35, 334–338.

Screen, H.R.C., Lee, D.A., Bader, D.L., Shelton, J.C., 2004. An investigation into the effects of the hierarchical structure of tendon fascicles on micromechanical properties. Proc. Inst. Mech. Eng. H 218, 109–119.

Seynnes, O.R., Bojsen-Moller, J., Albracht, K., Arndt, A., Cronin, N.J., Finni, T., Magnusson, S.P., 2015. Ultrasound-based testing of tendon mechanical properties: a critical evaluation. J. Appl. Physiol. 118, 133–141.

Seynnes, O.R., Erskine, R.M., Maganaris, C.N., Longo, S., Simoneau, E.M., Grosset, J.F., Narici, M.V., 2009. Training-induced changes in structural and mechanical properties of the patellar tendon are related to muscle hypertrophy but not to strength gains. J. Appl. Physiol. 107, 523–530.

Seynnes, O.R., Kamandulis, S., Kairaitis, R., Helland, C., Campbell, E.-L., Brazaitis, M., Skurvydas, A., Narici, M.V., 2013. Effect of androgenic-anabolic steroids and heavy strength training on patellar tendon morphological and mechanical properties. J. Appl. Physiol. 115, 84–89.

Seynnes, O.R., Koesters, A., Gimpl, M., Reifberger, A., Niederseer, D., Niebauer, J., Pirich, C., Muller, E., Narici, M.V., 2011. Effect of alpine skiing training on tendon mechanical properties in older men and women. Scand. J. Med. Sci. Spor. 21 Suppl 1, 39–46.

Shepherd, J.H., Screen, H.R.C., 2013. Fatigue loading of tendon. Int. J. Exp. Pathol. 94, 260–270.

Stafilidis, S., Arampatzis, A., 2007. Muscle - tendon unit mechanical and morphological properties and sprint performance. J. Sports Sci. 25, 1035–1046.

Wiesinger, H.-P., Rieder, F., Kösters, A., Müller, E., Seynnes, O.R., 2016. Are Sport-Specific Profiles of Tendon Stiffness and Cross-Sectional Area Determined by Structural or Functional Integrity? PLoS ONE 11, e0158441.

Woo, S.L., Ritter, M.A., Amiel, D., Sanders, T.M., Gomez, M.A., Kuei, S.C., Garfin, S.R., Akeson, W.H., 1980. The biomechanical and biochemical properties of swine tendons--long term effects of exercise on the digital extensors. Connect. Tissue Res. 7, 177–183.

Wren, T.A.L., Lindsey, D.P., Beaupré, G.S., Carter, D.R., 2003. Effects of creep and cyclic loading on the mechanical properties and failure of human Achilles tendons. Ann. Biomed. Eng. 31, 710–717.

Zavatsky, A.B., Beard, D.J., O'Connor, J.J., 1994. Cruciate Ligament Loading During Isometric Muscle Contractions: A Theoretical Basis for Rehabilitation. Am. J. Sports Med. 22, 418–423.

Figure captions

Figure 1 Schematic representation of the experimental setup and ultrasound analysis. Dynamometry (1) and kinematic recordings (2) were used to calculate knee joint moments based on an inverse dynamics approach. Electromyographic activity of the biceps femoris and gastrocnemius medialis (3) was recorded because of their contribution to the resultant knee joint moment and tibio-femoral movement, respectively. Ultrasound imaging was integrated to assess patellar tendon elongation (4). In the ultrasound image (panel A), the crosses indicate the tracking landmarks for the elongation measurement at the deep insertion at the apex of the patella, the tibial tuberosity and the tibia plateau. Only the displacement in the longitudinal axis of the tendon (upper dashed line) was considered in the elongation-measurement at the tibia plateau (arrow). The change of the angle (α) between the lower border of the patellar tendon and the anterior intercondylar area was used as an indication of tibia tilt during contractions. Panel B illustrates that the use of a tracking landmark at the tibia plateau is associated with a measurement bias (see vertical arrow heads) in case of sagittal plane rotation of the tibia. In the schematic, a rotation around the tendon insertion point at the tuberosity is assumed for simplification. The grey lines and the black lines represent the contours of the bones and the position of the tracking landmarks before and during contraction, respectively.

Figure 2 Mean and standard error (error bars) of the angle between the patellar tendon and anterior intercondylar area (see also figure 1) – used as an indication for tibia tilt – as a function of tendon force (relative to maximum tendon force exerted during a maximum voluntary contraction) and using a distal (white) or proximal (black) dynamometer shank pad position.

Figure 3 Patellar tendon force-elongation relationship (mean ± standard error of elongation) derived from isometric knee extension contractions with a dynamometer shank pad position either proximal (black) or distal (white) and using either the tibial tuberosity (triangles) or tiba plateau (circles) as tracking landmark in the evaluation of tendon elongation. # significant main effect of tracking landmark; ‡ significant main effect of force level; significant landmark-by-force level interaction; * significant post hoc difference between tracking landmarks; $p < 0.05$.

Figure 4 Tendon stiffness as first derivative of the force-elongation curve in 10%-intervals of maximum tendon force using either the tibial tuberosity (triangles) or tiba plateau (circles) as tracking landmark point in the evaluation of tendon elongation. Due to the absence of a significant main effect of pad position or pad position-by-force level interaction, data was collated for clarity. # significant main effect of tracking landmark; ‡ significant main effect of force level; significant landmark-by-force level interaction; * significant post hoc difference between tracking landmarks; $p < 0.05$.

Figure 5 Maximum tendon strain (A) and tendon stiffness (B) obtained from isometric ramp contractions with a distal (white) and proximal (black) dynamometer shank pad position and using either the tibial tuberosity or tiba plateau as tracking landmark in the evaluation of tendon elongation. Tendon strain was evaluated at the common maximum tendon force achieved during five ramp contractions and tendon stiffness was calculated between 50% of maximum MVC tendon force and the common maximum during the ramp contractions. # significant main effect of tracking landmark; † significant landmark- by-pad position interaction, indicating significantly greater differences between landmarks at the proximal pad position and between pad positions when using tibia plateau as tracking landmark; $p < 0.05$.

Figure 6 Bland and Altman plots illustrating the agreement between the use of the tibal tuberosity or plateau as tracking landmarks in the assessment of patellar tendon strain (A, B) and stiffness (C, D), and using a distal (white) or proximal (black) dynamometer shank pad position for the isometric contractions. The abscissa shows the absolute values for strain and stiffness averaged between reference points, the ordinate shows the differences between the values measured using the tuberosity (T) and plateau (P) as tracking landmark. The horizontal solid line shows the mean difference between landmarks; the dashed lines show the mean difference ± 1.96SD.

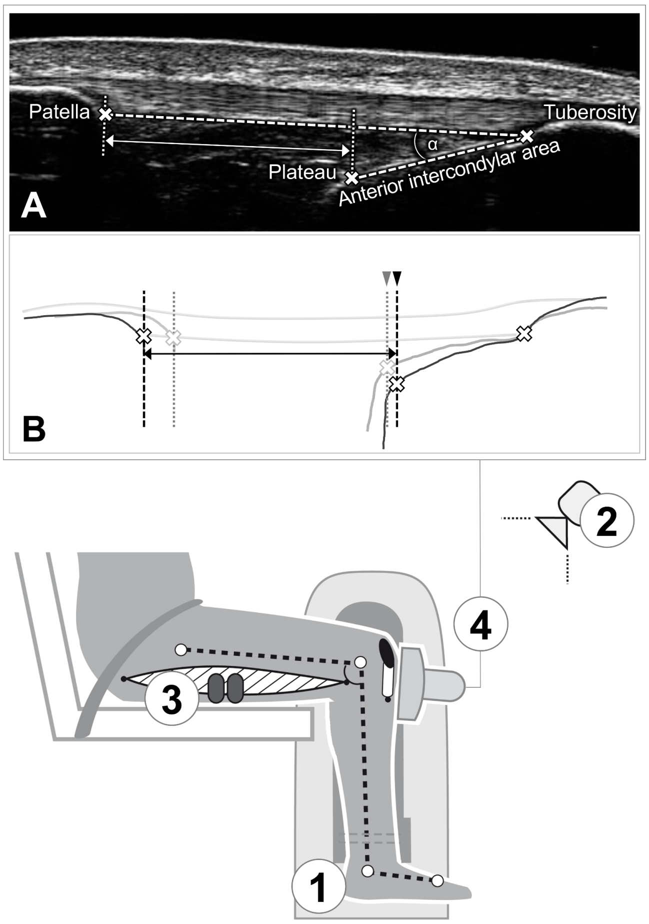

Patella
Tuberosity
α
Plateau
Anterior intercondylar area
A
B
2
4
3
1

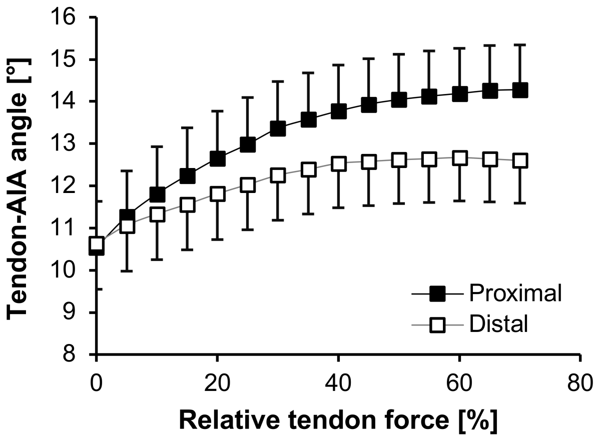
Tendon-AIA angle [°]
16
15
14
13
12
11
10
9
8
0
20
40
60
80
Relative tendon force [%]
Proximal
Distal

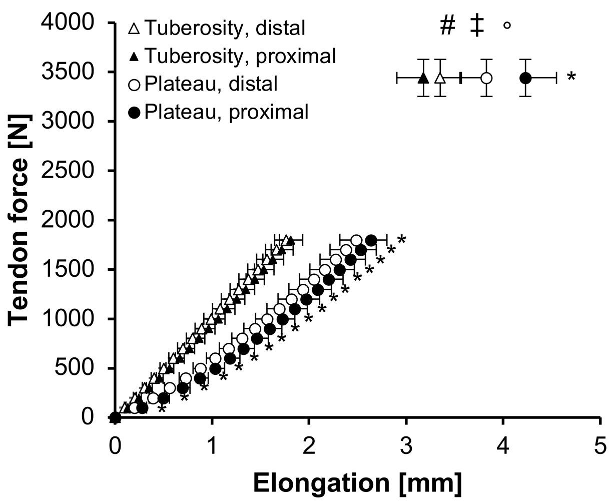
Tuberosity, distal
Tuberosity, proximal
Plateau, distal
Plateau, proximal
‡ °
*
Tendon force [N]
4000
3500
3000
2500
2000
1500
1000
500
0
0
1
2
3
4
5
Elongation [mm]

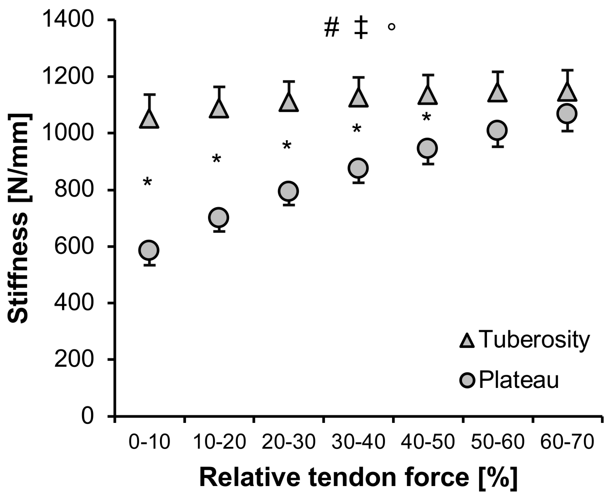

‡ °
1400
1200
1000
800
600
400
200
0
Stiffness [N/mm]
Tuberosity
Plateau
0-10
10-20
20-30
30-40
40-50
50-60
60-70
Relative tendon force [%]

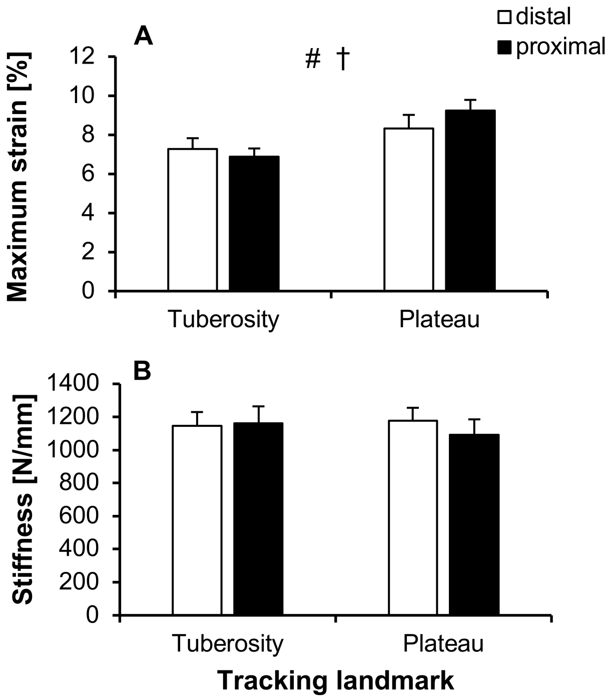

A
B
distal
proximal
†
Maximum strain [%]
0
2
4
6
8
10
12
Tuberosity
Plateau
Stiffness [N/mm]
0
200
400
600
800
1000
1200
1400
Tuberosity
Plateau
Tracking landmark

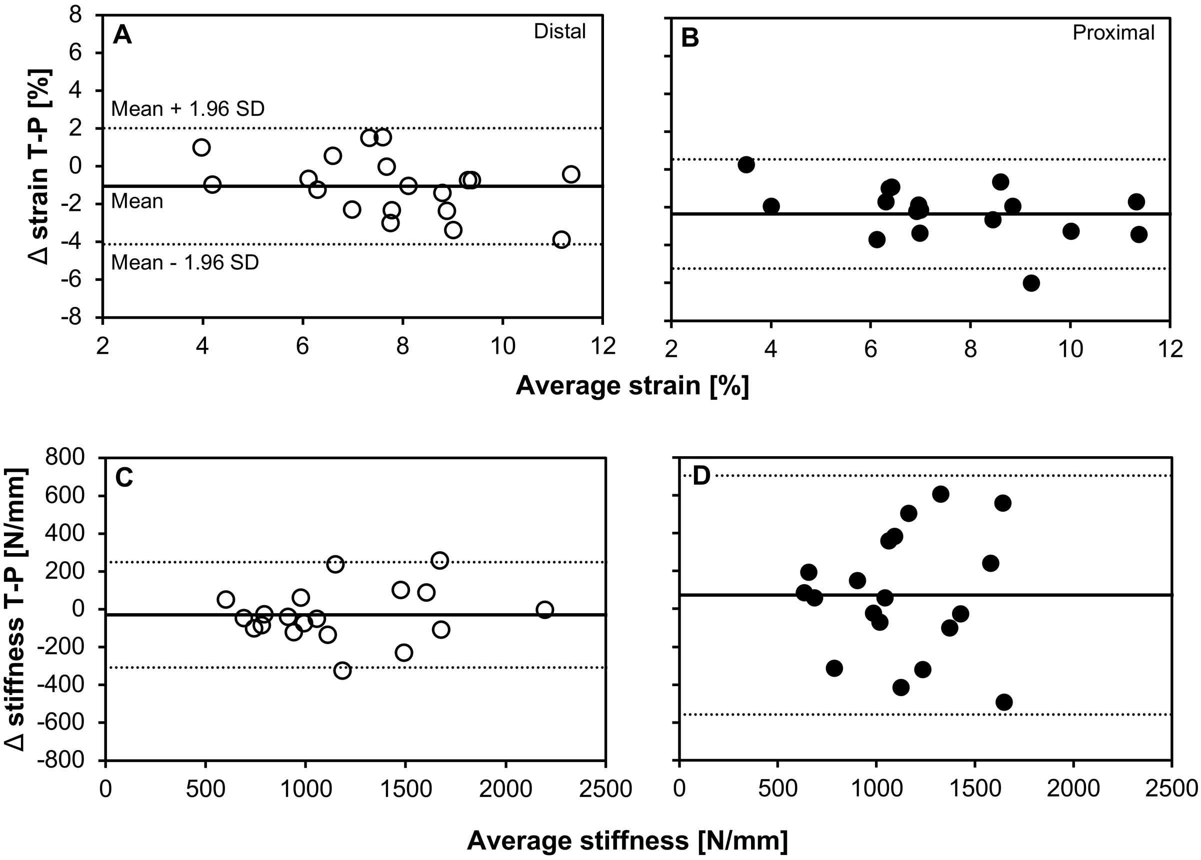

A
Distal
Mean + 1.96 SD
Mean
Mean - 1.96 SD
B
Proximal
Δ strain T-P [%]
Average strain [%]
C
D
Δ stiffness T-P [N/mm]
Average stiffness [N/mm]